Chapter 2
Linear Elastic Stress Analysis of 2D Cracks

Abstract To begin to understand fracture of materials, one must first know the stress and deformation fields near the tips of cracks. Thus the first topic in fracture mechanics is the linear elastic analysis of crack tip fields. The solutions derived here will be seen to violate the assumptions upon which linear elasticity theory is grounded. Nonetheless by invoking common sense principles, the theory of linear elastic fracture mechanics (LEFM) will be shown to provide the groundwork for many practical applications of fracture.

2.1 Notation

Unless otherwise stated all elastic analysis will be for static problems in linear elastic, isotropic, homogeneous materials in which no body forces act.

A *two dimensional* domain will be assumed to lie in the (x_1, x_2) plane and will be referred to as $\mathscr{A}$, with boundary curve $\mathscr{C}$ or Γ and outward unit normal vector $\mathbf{n}$. In a Cartesian coordinate system with basis vectors $\{\mathbf{e}_1, \mathbf{e}_2\}$, $\mathbf{n} = n_1\mathbf{e}_1 + n_2\mathbf{e}_2$, or $\mathbf{n} = n_\alpha \mathbf{e}_\alpha$ using the summation convention and the convention that Greek indices span 1, 2. An area integral will be denoted by $\int_{\mathscr{A}}(\cdot)dA$. A line integral is denoted by $\int_{\mathscr{C}\text{ or }\Gamma}(\cdot)d\Gamma$. New fracture surface area is referred to as $B \cdot da$, where B is the thickness of the 3D body that is idealized as 2D.

A three-dimensional domain will referred to as $\mathscr{V}$ with surface $\mathscr{S}$ and outward unit normal $\mathbf{n}$. The portion of the boundary over which tractions are prescribed is $\mathscr{S}_t$. The portion over which displacements are prescribed is $\mathscr{S}_u$. $\mathscr{S} = \mathscr{S}_t \bigcup \mathscr{S}_u$. In a Cartesian coordinate system with basis vectors $\{\mathbf{e}_1, \mathbf{e}_2, \mathbf{e}_3\}$, $\mathbf{n} = n_i\mathbf{e}_i$ where Latin indices span 1, 2, 3. A volume integral is denoted by $\int_{\mathscr{V}}(\cdot)dV$. A surface integral is denoted by $\int_{\mathscr{S}}(\cdot)dS$. New fracture surface area is referred to as ds or $\Delta\mathscr{S}$.

The stress tensor will be referred to as σ with components σ_{ij}. Strain is γ with components γ_{ij}. Traction $\mathbf{t} = \sigma\mathbf{n}$, or $t_i = \sigma_{ij}n_j$.

2.2 Introduction

Although real-world fracture problems involve crack surfaces that are curved and involve stress fields that are three dimensional, the only simple analyses that can

A.T. Zehnder, *Fracture Mechanics*,
Lecture Notes in Applied and Computational Mechanics 62,
DOI 10.1007/978-94-007-2595-9_2,

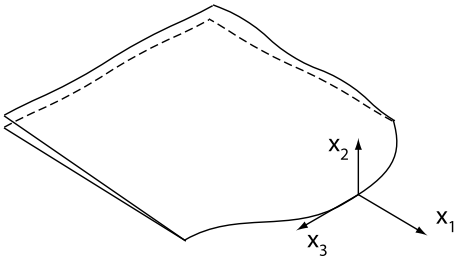

Fig. 2.1 Crack front, or line, for an arbitrarily shaped crack surface in a *solid*. At any point along the crack line a local coordinate system may be defined as shown

be performed are for two-dimensional idealizations. Solutions to these idealizations provide the basic structure of the crack tip fields.

Consider the arbitrary fracture surface shown in Fig. 2.1. At any point on the crack front a local coordinate system can be drawn with the x_3 axis tangential to the crack front, the x_2 axis orthogonal to the crack surface and x_1 orthogonal to the crack front. A polar coordinate system (r, θ) can be formed in the (x_1, x_2) plane. An observer who moves toward the crack tip along a path such that x_3 is constant will eventually be so close to the crack line front that the crack front appears to be straight and the crack surface flat. In such a case the three dimensional fracture problem at this point reduces to a two-dimensional one. The effects of the external loading and of the geometry of the problem are felt only through the magnitude and directions of the stress fields at the crack tip.

2.3 Modes of Fracture

At the crack tip the stress field can be broken up into three components, called Mode I, Mode II and Mode III, as sketched in Fig. 2.2, Mode I causes the crack to open orthogonal to the local fracture surface and results in tension or compressive stresses on surfaces that lie on the line $\theta = 0$ and that have normal vector $\mathbf{n} = \mathbf{e}_2$. Mode II causes the crack surfaces to slide relative to each other in the x_1 direction and results in shear stresses in the x_2 direction ahead of the crack. Mode-III causes the crack surface to slide relative to each other in the x_3 direction and results in shear stresses in the x_3 direction ahead of the crack.

With the idealization discussed above the solution of the crack tip fields can be broken down into three problems. Modes I and II are found by the solution of either a plane stress or plane strain problem and Mode III by the solution of an anti-plane shear problem.

2.4 Mode III Field

In many solid mechanics problems the anti-plane shear problem is the simplest to solve. This is also the case for fracture mechanics, thus we begin with this problem.

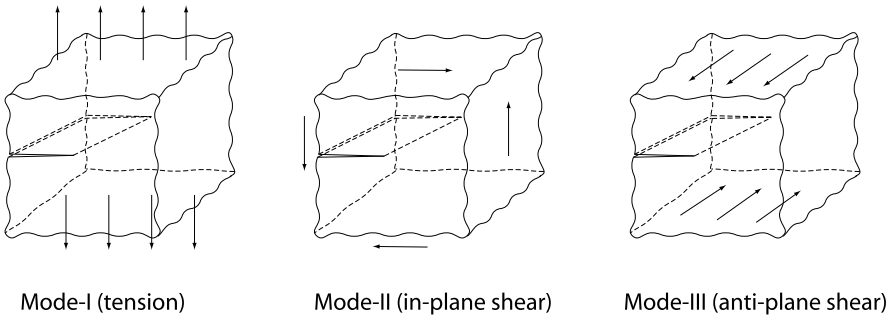

Fig. 2.2 Modes of fracture. Think of this as representing the state of stress for a cube of material surrounding part of a crack tip. The actual crack may have a mix of Mode-I,II,III loadings and this mix may vary along the crack front. The tractions on the front and back faces of Mode-III cube are not shown

Anti-plane shear is an idealization in which the displacement field is given by $\mathbf{u} = w(x_1, x_2)\mathbf{e}_3$. With this displacement field, the stress-strain relations are

$$\sigma_{3\alpha} = \mu w_{,\alpha}\,. \tag{2.1}$$

The field equations of linear elasticity reduce to

$$\nabla^2 w = 0 \tag{2.2}$$

on $\mathscr{A}$, with either traction boundary conditions,

$$\mu \nabla w \cdot \mathbf{n} = \sigma_{3\alpha} n_\alpha = \mu w_{,\alpha}\, n_\alpha = t_3^*(x_1, x_2) \tag{2.3}$$

or displacement boundary conditions,

$$w(x_1, w_2) = w^*(x_1, x_2) \tag{2.4}$$

on $\mathscr{C}$.

The anti-plane shear crack problem can be solved in two ways. In the first approach only the asymptotic fields near the crack tip are found. In the second, the entire stress field is found. Both solutions are given below.

2.4.1 Asymptotic Mode III Field

The geometry of the asymptotic problem is sketched in Fig. 2.3. An infinitely sharp, semi-infinite crack in an infinite body is assumed to lie along the x_1 axis. The crack surfaces are traction free.

This problem is best solved using polar coordinates, (r, θ). The field equation in polar coordinates is

$$\nabla^2 w = w_{,rr} + \frac{1}{r} w_{,r} + \frac{1}{r^2} w_{,\theta\theta} = 0, \tag{2.5}$$

Fig. 2.3 Semi-infinite crack in an infinite body. For clarity the crack is depicted with a small, but finite opening angle, actual problem is for a crack with no opening angle

and the traction free boundary conditions become

$$w_{,\theta}\,(r, \theta = \pm\pi) = 0. \tag{2.6}$$

Try to form a separable solution, $w(r, \theta) = R(r)T(\theta)$. Substituting into Eq. (2.5) and separating the r and θ dependent parts,

$$r^2 \frac{R''}{R} + r\frac{R'}{R} = -\frac{T''}{T} = \left\{ \begin{array}{c} \lambda^2 \\ 0 \\ -\lambda^2 \end{array} \right\}, \tag{2.7}$$

where λ is a scalar. If the RHS of Eq. (2.7) is $-\lambda^2$ or 0 a trivial solution is obtained. Thus the only relevant case is when the RHS $= \lambda^2$. In this case the following two differential equations are obtained

$$T'' + \lambda^2 T = 0, \tag{2.8}$$

$$r^2 R'' + r R' - \lambda^2 R = 0. \tag{2.9}$$

The first has the solution

$$T(\theta) = A\cos\lambda\theta + B\sin\lambda\theta. \tag{2.10}$$

The second has the solution

$$R(r) = r^{\pm\lambda}. \tag{2.11}$$

The boundary conditions, $w_{,\theta}\,(r, \theta = \pm\pi) = 0$ become $R(r)T'(\pm\pi) = 0$. This leads to the pair of equations

$$\lambda(-A\sin\lambda\pi + B\cos\lambda\pi) = 0, \tag{2.12}$$

$$\lambda(A\sin\lambda\pi + B\cos\lambda\pi) = 0. \tag{2.13}$$

Adding and subtracting these equations leads to two sets of solutions

$$B\lambda\cos\lambda\pi = 0, \quad \Rightarrow \quad \lambda = 0, \lambda = \pm\,1/2, \pm 3/2, \ldots, \tag{2.14}$$

$$A\lambda\sin\lambda\pi = 0, \quad \Rightarrow \quad \lambda = 0, \lambda = \pm 1, \pm 2, \ldots. \tag{2.15}$$

Thus the solution can be written as a series of terms. If $\lambda = 0$, then set $A = A_0$. Since $\lambda = 0$ corresponds to rigid body motion, set $B = 0$ when $\lambda = 0$ since it just adds to

the A_0 term. If $\lambda = \pm 1/2, \pm 3/2, \ldots$, then from Eq. (2.12) $A = 0$. If $\lambda = \pm 1, \pm 2$, then $B = 0$.

Assembling the terms yields

$$w(r,\theta) = \sum_{n=-\infty}^{n=+\infty} A_n r^n \cos n\theta + B_n r^{n+\frac{1}{2}} \sin(n+1/2)\theta. \tag{2.16}$$

Noting that the stress field in polar coordinates is given by

$$\sigma_{3r} = \mu \frac{\partial w}{\partial r}, \qquad \sigma_{3\theta} = \frac{\mu}{r} \frac{\partial w}{\partial \theta}, \tag{2.17}$$

Eq. (2.12) predicts that the stress field is singular, i.e. the stress becomes infinitely large as $r \to 0$. Naturally this will also mean that the strain becomes infinite at the crack tip thus violating the small strain, linear theory of elasticity upon which the result is based.

Various arguments are traditionally used to restrict the terms in Eq. (2.12) to $n \geq 0$ resulting in a maximum stress singularity of $\sigma \sim r^{-1/2}$.

One argument is that the strain energy in a finite region must be bounded. In anti-plane shear the strain energy density is $W = \frac{\mu}{2}(w,_1^2 + w,_2^2)$. If $w \sim r^\lambda$, then $W \sim r^{2\lambda-2}$. The strain energy in a circular region of radius R surrounding the crack tip is

$$\int_{\lim r_{\to 0}}^{R} \int_{-\pi}^{\pi} W r d\theta dr \sim R^{2\lambda} - \lim_{r\to 0} r^{2\lambda}.$$

Thus λ is restricted to $\lambda \geq 0$ for finite energy. From Eq. (2.12), $2\lambda = n$, or $n + 1/2$, thus if $\lambda \geq 0$ then we must restrict the series solution to $n \geq 0$.

A second argument is that the displacement must be bounded, which as with energy argument restricts the series to $n \geq 0$.

However, both of the above arguments assume the impossible, that the theory of linear elasticity is valid all the way to the crack tip despite the singular stresses. Even with the restriction that $n \geq 0$ the stress field is singular, thus since no material can sustain infinite stresses, there must exist a region surrounding the crack tip where the material yields or otherwise deforms nonlinearly in a way that relieves the stress singularity. If we don't claim that Eq. (2.12) must apply all the way to the crack tip, then outside of the crack tip nonlinear zone the energy and displacement will be finite for any order of singularity thus admitting terms with $n < 0$. Treating the crack tip nonlinear zone as a hole (an extreme model for material yielding in which the material's strength has dropped to zero) of radius ρ, Hui and Ruina [1] show that at any fixed, non-zero distance from the crack tip, the coefficients of terms with stresses more singular than $r^{-1/2}$ go to zero as $\rho/a \to 0$ where a is the crack length or other characteristic in-plane dimension such as the width of a test specimen or structural component. This result is in agreement with the restrictions placed on the crack tip fields by the energy and displacement arguments, thus in what follows the stress field is restricted to be no more singular than $\sigma \sim r^{-1/2}$. But note that in real-world problems in which the crack tip nonlinear zone is finite and $\rho/a \neq 0$,

the stress field outside the nonlinear zone will have terms more singular than $r^{-1/2}$. Further details of this calculation are given in Sect. 7.3 as a prototype model for the effects of crack tip plasticity on the stress fields.

Based on the above arguments, and neglecting crack tip nonlinearities, all terms in the displacement series solution with negative powers of r are eliminated, leaving as the first four terms:

$$w(r,\theta) = A_0 + B_0 r^{1/2} \sin\frac{\theta}{2} + A_1 r\cos\theta + B_2 r^{3/2}\sin\frac{3\theta}{2} + \cdots . \tag{2.18}$$

Since the problem is a traction boundary value problem, the solution contains a rigid body motion term, A_0.

The stress field in polar coordinates is calculated by substituting Eq. (2.18) into Eq. (2.17), yielding

$$\sigma_{3r} = B_0\mu\frac{1}{2}r^{-1/2}\sin\frac{\theta}{2} + A_1\mu\cos\theta + B_2\mu\frac{3}{2}r^{1/2}\sin\frac{3\theta}{2} + \cdots , \tag{2.19}$$

$$\sigma_{3\theta} = B_0\mu\frac{1}{2}r^{-1/2}\cos\frac{\theta}{2} - A_1\mu\sin\theta + B_2\mu\frac{3}{2}r^{1/2}\cos\frac{3\theta}{2} + \cdots . \tag{2.20}$$

Note that the stress field has a characteristic $r^{-1/2}$ singularity. It will be shown that this singularity occurs for the Mode I and Mode II problems as well.

As $r \to 0$ the $r^{-1/2}$ term becomes much larger than the other terms in the series and the crack tip stress field is determined completely by B_0, the amplitude of the singular term. By convention the amplitude of the crack tip singularity is called the Mode III stress intensity factor, K_{III}, and is defined as

$$K_{III} \equiv \lim_{r\to 0} \sigma_{3\theta}(r,0)\sqrt{2\pi r}. \tag{2.21}$$

Substituting Eq. (2.20) into the above, B_0 can be written as $B_0 = \sqrt{\frac{2}{\pi}}\frac{K_{III}}{\mu}$. Using the language of stress intensity factors, the first three terms of the series solution for the displacement and stress fields can be written as

$$w(r,\theta) = A_0 + \sqrt{\frac{2}{\pi}}\frac{K_{III}}{\mu}r^{1/2}\sin\frac{\theta}{2} + A_1 r\cos\theta + B_2 r^{3/2}\sin\frac{3\theta}{2} + \cdots \tag{2.22}$$

and

$$\begin{pmatrix}\sigma_{3r}\\ \sigma_{3\theta}\end{pmatrix} = \frac{K_{III}}{\sqrt{2\pi r}}\begin{pmatrix}\sin\frac{\theta}{2}\\ \cos\frac{\theta}{2}\end{pmatrix} + A_1\mu\begin{pmatrix}\cos\theta\\ -\sin\theta\end{pmatrix} + \frac{3B_2\mu r^{1/2}}{2}\begin{pmatrix}\sin\frac{3\theta}{2}\\ \cos\frac{3\theta}{2}\end{pmatrix}. \tag{2.23}$$

The stress intensity factor, K_{III} is not determined from this analysis. In general K_{III} will depend linearly on the applied loads and will also depend on the specific geometry of the cracked body and on the distribution of loads. There are a number approaches to calculating the stress intensity factor, many of which will be discussed later in this book.

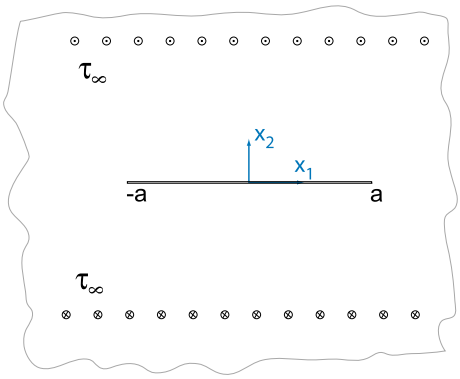

Fig. 2.4 Finite crack of length $2a$ in an infinite body under uniform anti-plane shear loading in the far field

2.4.2 Full Field for Finite Crack in an Infinite Body

A crack that is small compared to the plate dimension and whose shortest ligament from the crack to the outer plate boundary is much larger than the crack can be approximated as a finite crack in an infinite plate. If, in addition, the spatial variation of the stress field is not large, such a problem may be modeled as a crack of length $2a$ loaded by uniform shear stresses, $\sigma_{31} = 0, \sigma_{32} = \tau_\infty$, Fig. 2.4.

2.4.2.1 Complex Variables Formulation of Anti-Plane Shear

To simplify the notation the following definitions are made: $\tau_\alpha = \sigma_{3\alpha}, \gamma_\alpha = 2\gamma_{3\alpha}$. Let χ be a stress function such that

$$\tau_1 = -\frac{\partial \chi}{\partial x_2}, \quad \text{and} \quad \tau_2 = \frac{\partial \chi}{\partial x_1}. \tag{2.24}$$

From the strain-displacement relations $\gamma_\alpha = w_{,\alpha}$. Thus $\gamma_{1,2} = w_{,12}$ and $\gamma_{2,1} = w_{,21}$ from which the compatibility relation

$$\gamma_{1,2} = \gamma_{2,1} \tag{2.25}$$

is obtained. Using the stress strain relations, $\tau_\alpha = \mu\gamma_\alpha$, and the stress functions yields $\mu\gamma_{1,2} = -\chi_{,22}$ and $\mu\gamma_{2,1} = \chi_{,11}$. Substituting this into the compatibility equation yields $-\chi_{,22} = \chi_{,11}$ or

$$\nabla^2 \chi = 0. \tag{2.26}$$

Define a new, complex function using χ as the real part and w as the imaginary part,

$$h(z) = \chi + i\mu w \tag{2.27}$$

where $z = x_1 + ix_2$. It is easily verified that χ and w satisfy the Cauchy-Riemann equations. Furthermore both χ and w are harmonic, i.e. $\nabla^2\chi = 0$ and $\nabla^2 w = 0$,

thus h is an analytic function. Recall that the derivative of an analytic function, $f = u + iv$ is given by $f' = u,_1 + iv_1 = v,_2 - iu,_2$. Applying this rule to h yields $h' = \chi,_1 + i\mu w,_1$. Using the definition of the stress function and the stress-strain law it is seen that h' can be written as

$$h'(z) = \tau_2(z) + i\tau_1(z) \equiv \tau \tag{2.28}$$

where τ is called the complex stress.

A complex normal vector can also be defined, $n \equiv n_1 + in_2$. The product of τ and n is $\tau n = \tau_2 n_1 - \tau_1 n_2 + i(\tau_1 n_1 + \tau_2 n_2)$. Thus, comparing this expression to Eq. (2.3), the traction boundary conditions can be written as

$$\mathrm{Im}[\tau(z)n(z)] = t^*(z) \tag{2.29}$$

on $\mathscr{C}$.

2.4.2.2 Solution to the Problem

The problem to be solved is outlined in Fig. 2.4. A finite crack of length $2a$ lies along the x_1 axis. Far away from the crack a uniform shear stress field is applied, $\tau_1 = 0$, $\tau_2 = \tau_\infty$, or in terms of the complex stress, $\tau = \tau_\infty + i0$. The crack surfaces are traction free, i.e. $\mathrm{Re}[\tau] = \tau_2 = 0$ on $-a \le x_1 \le a$, $x_2 = 0$.

This problem can be solved by analogy to the solution for fluid flow around a flat plate, [2]. In the fluid problem the flow velocity v is given by $v = \overline{F'(z)}$, where $F = A(z^2 - a^2)^{1/2}$. With the fluid velocity analogous to the stress, try a solution of the form

$$h(z) = A(z^2 - a^2)^{1/2}. \tag{2.30}$$

It is easily shown that for $z \neq \pm a$ this function is analytic, thus the governing pde for anti-plane shear will be satisfied. All that remains is to check if the boundary conditions are satisfied. With the above h, the complex stress is

$$\tau = h'(z) = \frac{Az}{(z^2 - a^2)^{1/2}}. \tag{2.31}$$

As $z \to \infty$ $\tau \to A$, thus to satisfy the far-field boundary condition $A = \tau_\infty$.

To check if the crack tip is traction free note that in reference to Fig. 2.5 $z - a = r_1 e^{i\theta_1}$ and $z + a = r_2 e^{i\theta_2}$. Thus $z^2 - a^2 = r_1 r_2 e^{i(\theta_1 + \theta_2)}$.

On the top crack surface, $x_2 = 0^+$, $-a \le x_1 \le a$, $\theta_1 = \pi$ and $\theta_2 = 0$, thus $z^2 - a^2 = r_1 r_2 e^{i(\pi + 0)} = -r_1 r_2 = -a^2 + x_1^2$. Thus on this surface the complex stress is $\tau = \frac{\tau_\infty x_1}{\sqrt{-r_1 r_2}} = \frac{-i\tau_\infty x_1}{\sqrt{a^2 - x^2}}$. The traction free boundary condition on the top crack surface is $\mathrm{Im}[\tau n] = 0$ where $n = i$, thus the boundary condition can be written as $\mathrm{Re}[\tau] = 0$. Since the complex stress on the top fracture surface has only an imaginary part, the traction free boundary condition is shown to be satisfied.

On the bottom crack surface, $x_2 = 0^-$, $-a \le x_1 \le a$, $\theta_1 = \pi$ and $\theta_2 = 2\pi$, thus $z^2 - a^2 = r_1 r_2 e^{i(\pi + 2\pi)} = -r_1 r_2 = -a^2 + x_1^2$ and again the stress has no real part, thus showing that the traction free boundary conditions will be satisfied.

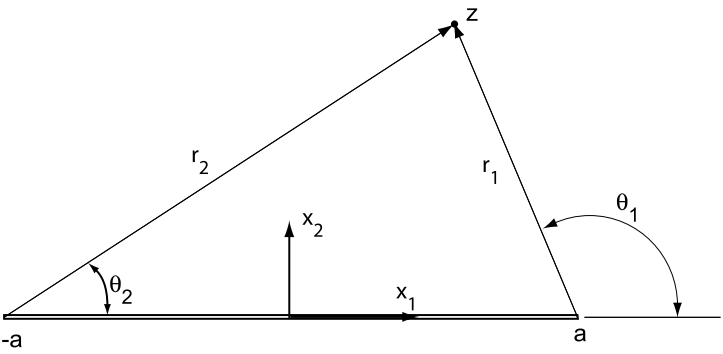

Fig. 2.5 Finite, antiplane-shear crack in an infinite body. θ_1 is discontinuous along $z = x_1, x_1 \geq a$. θ_2 is discontinuous along $z = x_1, x_1 \geq -a$

To summarize we have the following displacement and stress fields

$$w = \frac{1}{\mu}\,\mathrm{Im}[h] = \mathrm{Im}\,\frac{\tau_\infty}{\mu}\sqrt{(z^2 - a^2)}, \tag{2.32}$$

$$\tau = \tau_2 + i\,\tau_1 = \frac{\tau_\infty z}{\sqrt{z^2 - a^2}}. \tag{2.33}$$

Your intuition will tell you that near the crack tip this solution should give the same result as Eq. (2.23). To show that this is so, the stress field is analyzed near the right crack tip, $z \to a$. Note that $z^2 - a^2 = (z + a)(z - a)$. Setting $z \approx a$, $z^2 - a^2 \approx (z - a)(2a)$, hence near the right hand crack tip $\tau = \frac{\tau_\infty a}{\sqrt{z-a}\sqrt{2a}}$. Writing $z - a = r_1 e^{i\theta_1}$, and relabeling $\theta_1 = \theta$ the stress can be written as

$$\tau = \tau_2 + i\,\tau_1 = \frac{\tau_\infty\sqrt{a}}{\sqrt{2}\sqrt{r_1}}e^{-i\theta/2} = \frac{\tau_\infty\sqrt{a}}{\sqrt{2r_1}}\big(\cos\theta/2 - i\,\sin\theta/2\big) \quad \text{as } r_1 \to 0. \tag{2.34}$$

Comparing the above to Eq. (2.23) it is verified that near the crack tip the two stress fields are the same.

Note that unlike the asymptotic problem, the stress field in this problem is completely determined and the stress intensity factor can be determined. Recall the definition of the Mode-III stress intensity factor, Eq. (2.21) $K_{III} \equiv \lim_{r\to 0}\sigma_{3\theta}(r, 0)\sqrt{2\pi r}$. Noting that τ_2 is simply a shorthand notation for σ_{32}, and that r in the asymptotic problem is the same as r_1 in the finite crack problem, from Eq. (2.34)

$$K_{III} = \frac{\tau_\infty\sqrt{a}}{\sqrt{2r_1}}\sqrt{2\pi r_1} = \tau_\infty\sqrt{\pi a}. \tag{2.35}$$

Thus it is seen that the stress intensity factor scales as the applied load (τ_∞) and the square root of the crack length (a). As other problems are discussed it will be seen that such scaling arises again and again.

This scaling could have been deduced directly from the dimensions of stress intensity factor which are stress·length$^{1/2}$ or force/length$^{3/2}$. Since in this problem the only quantities are the applied stress and the crack length, the only way to combine them to produce the correct dimension for stress intensity factor is $\tau_\infty a^{1/2}$. See the exercises for additional examples.

Note as well that having the complete solution in hand one can check how close to the crack must one be for the asymptotic solution to be a good description of the actual stress fields. Taking the full solution, Eq. (2.33) to the asymptotic solution, Eq. (2.34) it can be shown, see exercises, that the asymptotic solution is valid in a region near the crack tips of $r \preceq a/10$.

2.5 Mode I and Mode II Fields

As with the Mode III field, the Mode I and Mode II problems can be solved either by asymptotic analysis or through the solution to a specific boundary value problem such as a finite crack in an infinite plate. However, as in the analysis above for the Mode III crack, the near crack tip stress fields are the same in each case. Thus the approach of calculating only the asymptotic stress fields will be taken here, following the analysis of Williams [3].

The Mode-I and Mode-II problems are sketched in Fig. 2.2. The coordinate system and geometry are the same as the Mode-III asymptotic problem, Fig. 2.3. Plane stress and plane strain are assumed.

2.5.1 Review of Plane Stress and Plane Strain Field Equations

2.5.1.1 Plane Strain

The plane strain assumption is that $u_3 = 0$ and $u_\alpha = u_\alpha(x_1, x_2)$. This assumption is appropriate for plane problems in which the loading is all in the x_1, x_2 plane and for bodies in which the thickness (x_3 direction) is much greater than the in-plane (x_1, x_2) dimensions. The reader can refer to an textbook on linear elasticity theory for the derivations of the following results:

$$\begin{aligned}
\gamma_{\alpha\beta} &= \frac{1}{2}(u_{\alpha,\beta} + u_{\beta,\alpha}),\\
\gamma_{\alpha\beta} &= \frac{1+\nu}{E}(\sigma_{\alpha\beta} - \nu\sigma_{\gamma\gamma}\delta_{\alpha\beta}),\\
\sigma_{\alpha\beta,\beta} &= 0,\\
\sigma_{33} &= \nu\sigma_{\gamma\gamma}.
\end{aligned}$$

2.5.1.2 Plane Stress

The plane stress assumption is that $\sigma_{33} = 0$ and that $u_\alpha = u_\alpha(x_1, x_2)$. This assumption is appropriate for plane problems in bodies that are thin relative to their in-plane dimensions. For example, the fields for crack in a plate of thin sheet metal loaded in tension could be well approximated by a plane stress solution. The strain-displacement and equilibrium equations are the same as for plane strain. The stress-strain law can be written as

$$\gamma_{33} = -\frac{\nu}{E}\sigma_{\gamma\gamma} = -\frac{\nu}{1-\nu}\gamma_{\gamma\gamma},$$
$$\gamma_{\alpha\beta} = \frac{1+\nu}{E}\left(\sigma_{\alpha\beta} - \frac{\nu}{1+\nu}\sigma_{\gamma\gamma}\delta_{\alpha\beta}\right).$$

2.5.1.3 Stress Function

To solve for the stress field one approach is to define and then solve for the stress function, Φ. In Cartesian coordinates the stresses are related to $\Phi(x_1, x_2)$ by

$$\sigma_{11} = \Phi_{,22}\,, \tag{2.36}$$
$$\sigma_{22} = \Phi_{,11}\,, \tag{2.37}$$
$$\sigma_{12} = -\Phi_{,12}\,. \tag{2.38}$$

In polar coordinates the stress is related to $\Phi(r, \theta)$ by

$$\sigma_{\theta\theta} = \Phi_{,rr}\,, \tag{2.39}$$
$$\sigma_{rr} = \frac{1}{r}\Phi_{,r} + \frac{1}{r^2}\Phi_{,\theta\theta}\,, \tag{2.40}$$
$$\sigma_{r\theta} = -\left(\frac{1}{r}\Phi_{,\theta}\right)_{,r}\,. \tag{2.41}$$

It is readily shown that stresses derived from such a stress function satisfy the equilibrium equations. Requiring the stresses to satisfy compatibility requires that Φ satisfies the biharmonic equation

$$\nabla^4\Phi = 0. \tag{2.42}$$

In polar coordinates this can be written as $\nabla^4\Phi = \nabla^2(\nabla^2\Phi)$, $\nabla^2\Phi = \Phi_{,rr} + \frac{1}{r}\Phi_{,r} + \frac{1}{r^2}\Phi_{,\theta\theta}$.

2.5.2 Asymptotic Mode I Field

2.5.2.1 Stress Field

The asymptotic crack problem is the same as that shown in Fig. 2.3. The traction free boundary conditions, $\mathbf{t} = 0$ on $\theta = \pm\pi$ require that $\sigma_{\theta\theta} = \sigma_{r\theta} = 0$ on $\theta = \pm\pi$. In

terms of the stress function the boundary conditions are $\Phi_{,rr} = 0$ and $(\frac{1}{r}\Phi_{,\theta})_{,r} = 0$ on $\theta = \pm\pi$.

Following Williams's approach [3] consider a solution of the form

$$\Phi(r,\theta) = r^{\lambda+2}\big[A\cos\lambda\theta + B\cos(\lambda+2)\theta\big] + r^{\lambda+2}\big[C\sin\lambda\theta + D\sin(\lambda+2)\theta\big]. \tag{2.43}$$

Note that one could start from a more basic approach. For example the general solution to the biharmonic equation in polar coordinates, found in 1899 by Michell and given in Timoshenko and Goodier [4] could be used as a starting point. Only certain terms of this result, corresponding to those used by Williams, will be needed to satisfy the boundary conditions of the crack problem.

It will be noted that the first two terms of Eq. (2.43) are symmetric with respect to the crack line and that the second two are anti-symmetric with respect to the crack. It will be shown that these correspond to the solutions of the Mode-I and Mode-II problems respectively. Let us consider for now, only the Mode-I solution. The boundary condition $\Phi, rr = 0$ on $\pm\pi$ (normal component of traction) yields

$$\Phi_{,rr}|_{\pi} = (\lambda+2)(\lambda+1)r^{\lambda}\big[A\cos\lambda\pi + B\cos(\lambda+2)\pi\big] = 0.$$

Noting that $\cos(\lambda\pi + 2\pi) = \cos\lambda\pi$, the above requires (for a nontrivial solution) that

$$(\lambda+2)(\lambda+1)(A+B)\cos\lambda\pi = 0. \tag{2.44}$$

The requirement that the shear component of traction is zero, yields

$$\left(\frac{1}{r}\Phi_{,\theta}\right)_{,r}\Bigg|_{\pi} = (\lambda+1)r^{\lambda}\big[-A\lambda\sin\lambda\pi - B(\lambda+2)\sin(\lambda\pi+2\pi)\big] = 0.$$

This leads to

$$\sin\lambda\pi\big[A\lambda + B(\lambda+2)\big]. \tag{2.45}$$

If the stress function is $\Phi \sim r^{\lambda+2}$, then the stress will be $\sigma \sim r^{\lambda}$, and since stress and strain are proportional to the first derivatives of the displacement, the displacement fields will be $u \sim r^{\lambda+1}$, $\lambda \neq -1$ or $u \sim \ln r$, $\lambda = -1$. As in the anti-plane shear problem, a reasonable assumption is that the displacements at the crack tip will be finite. This will restrict the solution to $\lambda > -1$.

To satisfy Eqs. (2.44) and (2.45) requires that

$$\cos\lambda\pi = 0 \quad\Rightarrow\quad \lambda = -\frac{1}{2}, \frac{1}{2}, \frac{3}{2}, \ldots, \quad \text{and} \quad B = -\lambda A/(\lambda+2),$$

or

$$\sin\lambda\pi = 0 \quad\Rightarrow\quad \lambda = 0, 1, 2, \ldots, \quad \text{and} \quad B = -A.$$

Taking the first three terms of the solution, for $\lambda = -\frac{1}{2}$, $B_{-1/2} = \frac{1}{3}A_{-1/2}$, for $\lambda = 0$, $B_0 = -A_0$ and for $\lambda = 1/2$, $B_{1/2} = -\frac{1}{5}A_{1/2}$. Thus the stress function is

$$\Phi(r,\theta) = r^{3/2}A_{-1/2}\left[\cos\frac{\theta}{2} + \frac{1}{3}\cos\frac{3\theta}{2}\right] + r^2 A_0[1-\cos 2\theta] + r^{5/2}A_{1/2}\left[\cos\frac{\theta}{2} - \frac{1}{5}\cos\frac{5\theta}{2}\right] + \text{H.O.T.} \tag{2.46}$$

Taking the derivative $\Phi_{,rr}$, the "hoop stress", $\sigma_{\theta\theta}$ is

$$\sigma_{\theta\theta} = \frac{3}{4}A_{-1/2}r^{-1/2}\left[\cos\frac{\theta}{2} + \frac{1}{3}\cos\frac{3\theta}{2}\right] + 2A_0\left[1-\cos 2\theta\right] + \frac{1}{4}A_{1/2}r^{1/2}\left[15\cos\frac{\theta}{2} - 3\cos\frac{5\theta}{2}\right] + \text{H.O.T.}$$

As in the anti-plane shear problem, the crack tip stress field is infinite with a $1/\sqrt{r}$ singularity. The strength of this singularity is given by the "Mode-I" stress intensity factor, K_I. By definition,

$$K_I \equiv \lim_{r\to 0}\sigma_{\theta\theta}|_{\theta=0}\sqrt{2\pi r} = A_{-1/2}\sqrt{2\pi}. \tag{2.47}$$

Replacing $A_{-1/2}$ by $K_I/\sqrt{2\pi}$ the stress function can be written as

$$\Phi(r,\theta) = \frac{K_I}{\sqrt{2\pi}}r^{3/2}\left[\cos\frac{\theta}{2} + \frac{1}{3}\cos\frac{3\theta}{2}\right] + 2A_0 r^2[1-\cos 2\theta] + r^{5/2}A_{1/2}\left[\cos\frac{\theta}{2} - \frac{1}{5}\cos\frac{5\theta}{2}\right] + \text{H.O.T.} \tag{2.48}$$

Taking derivatives of the stress function, the stress field can be written as

$$\begin{pmatrix}\sigma_{rr}\\ \sigma_{\theta\theta}\\ \sigma_{r\theta}\end{pmatrix} = \frac{K_I}{\sqrt{2\pi r}}\frac{1}{4}\begin{pmatrix}-\cos\frac{3\theta}{2} + 5\cos\frac{\theta}{2}\\ \cos\frac{3\theta}{2} + 3\cos\frac{\theta}{2}\\ \sin\frac{\theta}{2} + \sin\frac{3\theta}{2}\end{pmatrix} + 4A_0\begin{pmatrix}\cos^2\theta\\ \sin^2\theta\\ -\sin\theta\cos\theta\end{pmatrix} + \frac{3A_{1/2}r^{1/2}}{4}\begin{pmatrix}3\cos\frac{\theta}{2} + \cos\frac{5\theta}{2}\\ 5\cos\frac{\theta}{2} - \cos\frac{5\theta}{2}\\ \sin\frac{\theta}{2} - \sin\frac{5\theta}{2}\end{pmatrix} + \text{H.O.T.} \tag{2.49}$$

2.5.2.2 Displacement Field

Finding the displacement field can be a more difficult problem than finding the stress field. One approach is to calculate the strains using the stress-strain laws,

and then integrate the strain-displacement relations to determine the displacement fields. Williams used the approach of starting from the solution of Coker and Filon [5] in which it is shown that the displacement components in polar coordinates are related to the stress function by

$$2\mu u_r = -\Phi_{,r} + (1-\overline{\nu}) r \Psi_{,\theta}\,, \tag{2.50}$$

$$2\mu u_\theta = -\frac{1}{r}\Phi_{,\theta} + (1-\overline{\nu}) r^2 \Psi_{,r} \tag{2.51}$$

where the displacement potential, Ψ is related to the stress function by

$$\nabla^2 \Phi = (r\Psi_{,\theta})_{,r}\,, \tag{2.52}$$

μ is the shear modulus, and $\overline{\nu} = \nu$ for plane strain and $\overline{\nu} = \nu/(1+\nu)$ for plane stress.

As above, the (Mode-I) stress function is a power series in r. Assume that the displacement potential can also we written as a power series, thus we have

$$\Phi(r,\theta) = r^{\lambda+2}[A\cos\lambda\theta + B\cos(\lambda+2)\theta], \tag{2.53}$$

$$\Psi(r,\theta) = r^m[a_1\cos m\theta + a_2 \sin m\theta]. \tag{2.54}$$

Evaluating the derivatives of Eq. (2.53) and substituting into Eq. (2.52) yields $a_1 = 0$, $a_2 = 4A/\lambda$ and $m = \lambda$. Thus the terms of the Mode-I displacement potential are

$$\Psi = r^\lambda \frac{4A}{\lambda}\sin\lambda\theta. \tag{2.55}$$

Taking only the first term of the series (corresponding to $\lambda = -1/2$),

$$\Phi = A_{-1/2} r^{3/2}\left[\cos\frac{\theta}{2} + \frac{1}{3}\cos\frac{3\theta}{2}\right], \tag{2.56}$$

$$\Psi = 8A_{-1/2} r^{-1/2}\sin\frac{\theta}{2}. \tag{2.57}$$

Substituting into Eq. (2.50) and replacing $A_{-1/2}$ by $K_I/\sqrt{2\pi}$ yields

$$\begin{pmatrix} u_r \\ u_\theta \end{pmatrix} = K_I \frac{(1+\nu)}{E}\sqrt{\frac{r}{2\pi}}\begin{pmatrix} (\frac{5}{2} - 4\overline{\nu})\cos\frac{\theta}{3} - \frac{1}{2}\cos\frac{3\theta}{2} \\ -(\frac{7}{2} - 4\overline{\nu})\sin\frac{\theta}{2} + \frac{1}{2}\sin\frac{3\theta}{2} \end{pmatrix}. \tag{2.58}$$

The shape of the crack under load is a parabola, as can be found by considering the opening displacement of the crack, $u_2(r,\pm\pi) = -u_\theta(r,\pm\pi)$:

$$u_2(r,\pm\pi) = -u_\theta(r,\pm\pi) = \pm\frac{4K_I}{E'}\sqrt{\frac{r}{2\pi}} \tag{2.59}$$

where $E' = E$ for plane stress and $E' = \frac{E}{1-\nu^2}$ for plane strain.

2.5.3 Asymptotic Mode II Field

The details of the Mode II solution will not be given as the steps are identical to those taken for the Mode I solution. The resulting stress and displacement fields are expressed in terms of the Mode-II stress intensity factor, K_{II}, defined as

$$K_{II} \equiv \lim_{r\to 0} \sigma_{r\theta}|_{\theta=0}\sqrt{2\pi r}. \tag{2.60}$$

The first term of the stress field is given by

$$\begin{pmatrix}\sigma_{rr}\\ \sigma_{\theta\theta}\\ \sigma_{r\theta}\end{pmatrix} = \frac{K_{II}}{\sqrt{2\pi r}}\frac{1}{4}\begin{pmatrix}-5\sin\frac{\theta}{2}+3\sin\frac{3\theta}{2}\\ -3\sin\frac{\theta}{2}-3\sin\frac{3\theta}{2}\\ \cos\frac{\theta}{2}+3\cos\frac{3\theta}{2}\end{pmatrix}. \tag{2.61}$$

The displacement field is given by

$$\begin{pmatrix}u_r\\ u_\theta\end{pmatrix} = K_{II}\frac{(1+\nu)}{E}\sqrt{\frac{r}{2\pi}}\begin{pmatrix}(-\frac{5}{2}+4\overline{\nu})\sin\frac{\theta}{2}+\frac{3}{2}\sin\frac{3\theta}{2}\\ -(\frac{7}{2}-4\overline{\nu})\cos\frac{\theta}{2}+\frac{3}{2}\cos\frac{3\theta}{2}\end{pmatrix}. \tag{2.62}$$

2.6 Complex Variables Method for Mode I and Mode II Cracks

To determine the full stress field for a finite Mode-I or Mode-II crack we will need to use the method of complex variables. The solution we develop will allows us to find the stress and displacement fields as well as the stress intensity factors for any loading of a finite crack in an infinite plate. We consider a crack of length $2a$ lying along $x_2 = 0$, as shown in Fig. 2.5.

Following Hellan [6], the biharmonic equation (2.42) $\nabla^4\Phi = 0$, is solved by

$$2\Phi = \mathrm{Re}\big[\bar{z}\phi(z) + \psi(z)\big], \tag{2.63}$$

where ϕ and ψ are analytic functions of $z = x_1 + ix_2$. The stresses are given by

$$\sigma_{11} = \mathrm{Re}\left[\phi' - \frac{1}{2}\bar{z}\phi'' - \frac{1}{2}\psi''\right], \tag{2.64}$$

$$\sigma_{22} = \mathrm{Re}\left[\phi' + \frac{1}{2}\bar{z}\phi'' + \frac{1}{2}\psi''\right], \tag{2.65}$$

$$\sigma_{12} = \frac{1}{2}\,\mathrm{Im}\big[\bar{z}\phi'' + \psi''\big]. \tag{2.66}$$

The displacements can be found from

$$4\mu u_1 = \mathrm{Re}\big[\kappa\phi - \bar{z}\phi' - \psi'\big], \tag{2.67}$$

$$4\mu u_2 = \mathrm{Im}\big[\kappa\phi + \bar{z}\phi' + \psi'\big], \tag{2.68}$$

where $\kappa = 3 - 4\nu$ for plane strain and $\kappa = (3-\nu)/(1+\nu)$ for plane stress.

The fracture problems can be broken up into Mode-I (symmetric) and Mode-II (anti-symmetric) problems. To simplify the calculations the results above can be specialized to the two cases using the Westergaard approach [7].

2.6.1 Westergaard Approach for Mode-I

For the Mode-I case, along $x_2 = 0$ $\sigma_{12} = 0$, which can be enforced by setting $\psi'' = -z\phi''$. In this case $\psi' = -z\phi' + \phi + \text{const.}$ and the stresses can be written as

$$\begin{aligned} \sigma_{11} &= \operatorname{Re}\phi' - x_2 \operatorname{Im}\phi'', \\ \sigma_{22} &= \operatorname{Re}\phi' + x_2 \operatorname{Im}\phi'', \\ \sigma_{12} &= -x_2 \operatorname{Re}\phi''. \end{aligned} \tag{2.69}$$

The displacements are

$$\begin{aligned} 2\mu u_1 &= \frac{\kappa - 1}{2} \operatorname{Re}\phi - x_2 \operatorname{Im}\phi', \\ 2\mu u_2 &= \frac{\kappa + 1}{2} \operatorname{Im}\phi - x_2 \operatorname{Re}\phi'. \end{aligned} \tag{2.70}$$

2.6.2 Westergaard Approach for Mode-II

For Mode-II, along $x_2 = 0$ $\sigma_{22} = 0$ which can be enforced by setting $\psi'' = -2\phi' - z\phi''$. In this case $\psi' = -\phi - z\phi' + \text{const.}$ The stresses are

$$\begin{aligned} \sigma_{11} &= 2\operatorname{Re}\phi' - x_2 \operatorname{Im}\phi'', \\ \sigma_{22} &= x_2 \operatorname{Im}\phi'', \\ \sigma_{12} &= -\operatorname{Im}\phi' - x_2 \operatorname{Re}\phi''. \end{aligned} \tag{2.71}$$

The displacements are

$$\begin{aligned} 2\mu u_1 &= \frac{\kappa + 1}{2} \operatorname{Re}\phi - x_2 \operatorname{Im}\phi', \\ 2\mu u_2 &= \frac{\kappa - 1}{2} \operatorname{Im}\phi - x_2 \operatorname{Re}\phi'. \end{aligned} \tag{2.72}$$

2.6.3 General Solution for Internal Crack with Applied Tractions

If the crack surfaces have traction loading $\mathbf{t} = p_1(x_1)\mathbf{e}_1 + p_2(x_1)\mathbf{e}_2$ on the top surface and equal but opposite tractions on the bottom surface, as shown in Fig. 2.6 Sedov [8] gives the following general solutions for ϕ'.

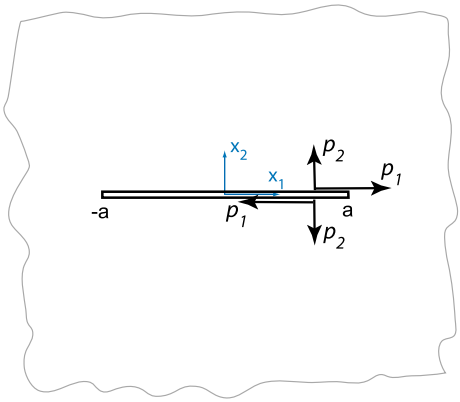

Fig. 2.6 Traction on crack face

For Mode-I,

$$\phi' = \frac{1}{\pi\sqrt{z^2 - a^2}} \int_{-a}^{a} p_2(t) \frac{\sqrt{a^2 - t^2}}{z - t}\, dt. \tag{2.73}$$

For Mode-II,

$$\phi' = \frac{-i}{\pi\sqrt{z^2 - a^2}} \int_{-a}^{a} p_1(t) \frac{\sqrt{a^2 - t^2}}{z - t}\, dt. \tag{2.74}$$

2.6.4 Full Stress Field for Mode-I Crack in an Infinite Plate

The stress and displacement fields for a finite crack subject to uniform tension loading, $\sigma_{22} = \sigma_\infty$, $\sigma_{11} = 0$, and $\sigma_{12} = 0$ can now be calculated using the above method. A superposition approach is taken as sketched in Fig. 2.7. If no crack were present, than along $x_2 = 0$ there would be a tensile stress of $\sigma_{22} = \sigma^\infty$. To make the crack traction free we apply a compressive stress to the crack faces, i.e. on the upper crack face apply $p_2 = \sigma_\infty$. The solution to the problem is the superposition of the uniform stress $\sigma_{22} = \sigma_\infty$ with the stress due to the crack face loadings.

For the crack face loading part of the problem,

$$\phi' = \frac{\sigma_\infty}{\pi\sqrt{z^2 - a^2}} \int_{-a}^{a} \frac{\sqrt{a^2 - t^2}}{z - t}\, dt. \tag{2.75}$$

Evaluating this integral yields

$$\phi' = \frac{\sigma_\infty z}{\sqrt{z^2 - a^2}} - \sigma_\infty, \tag{2.76}$$

which can be integrated to yield

$$\phi = \sigma_\infty\sqrt{z^2 - a^2} - \sigma_\infty z + \text{const.} \tag{2.77}$$

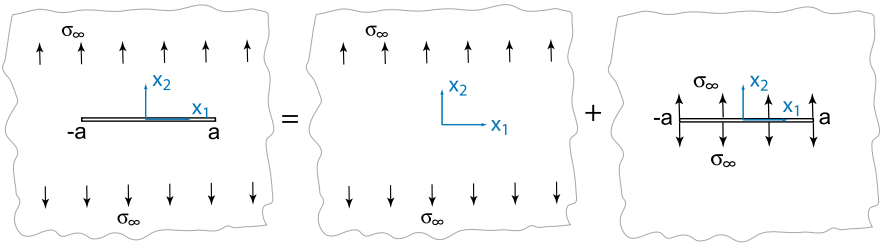

Fig. 2.7 Crack of length $2a$ in an infinite plate with far field stress $\sigma_{22} = \sigma_\infty$. Problem can be solved by superposition of uniform stress and crack in plate with no far field loading but with crack face pressures equal to σ_∞

Superposing the uniform far-field stress with the stress given by the stress functions, Eq. (2.69), yields $\sigma_1 = \mathrm{Re}\,\phi' - x_2\,\mathrm{Im}\,\phi''$, $\sigma_{22} = \mathrm{Re}\,\phi' + x_2\,\mathrm{Im}\,\phi'' + \sigma_\infty$ and $\sigma_{12} = -x_2\,\mathrm{Re}\,\phi''$. Substituting in ϕ' from Eq. (2.76) yields

$$\begin{aligned}
\sigma_{11} &= \sigma_\infty\left[\mathrm{Re}\left(\frac{z}{\sqrt{z^2-a^2}}\right) - x_2\,\mathrm{Im}\left(\frac{1}{\sqrt{z^2-a^2}} - \frac{z^2}{(z^2-a^2)^{3/2}}\right)\right] - \sigma_\infty,\\
\sigma_{22} &= \sigma_\infty\left[\mathrm{Re}\left(\frac{z}{\sqrt{z^2-a^2}}\right) + x_2\,\mathrm{Im}\left(\frac{1}{\sqrt{z^2-a^2}} - \frac{z^2}{(z^2-a^2)^{3/2}}\right)\right], \qquad (2.78)\\
\sigma_{12} &= -\sigma_\infty x_2\,\mathrm{Re}\left(\frac{1}{\sqrt{z^2-a^2}} - \frac{z^2}{(z^2-a^2)^{3/2}}\right).
\end{aligned}$$

Evaluating the stresses along $z = x_1$:

$$\begin{aligned}
\sigma_{11}(x_1,0) &= \mathrm{Re}\left(\frac{\sigma_\infty x_1}{\sqrt{x_1^2-a^2}}\right) - \sigma_\infty,\\
\sigma_{22}(x_1,0) &= \mathrm{Re}\left(\frac{\sigma_\infty x_1}{\sqrt{x_1^2-a^2}}\right),\\
\sigma_{12}(x_1,0) &= 0.
\end{aligned}$$

Note that along the crack line, for $-a \le x_1 \le a$, $\mathrm{Re}(\frac{\sigma_\infty x_1}{\sqrt{x_1^2-a^2}}) = 0$, and hence $\sigma_{22} = 0$ as required, and $\sigma_{11} = -\sigma_\infty$. Along the crack the plate is in compression in the x_1 direction, which can lead to local buckling when large, thin, cracked sheets are loaded in tension. Using Eqs. (2.78) the stress fields σ_{11} and σ_{22}, normalized by σ_∞, are plotted in Fig. 2.8 for $0 \le x_1/a \le 2$, $0 \le x_2/a \le 1$.

We can determine the stress intensity factor by examining the solution near one of the crack tips. Let $r = x_1 - a$, $x_1 = r + a$ then as $r \to 0$, i.e. near the right hand crack tip

$$\sigma_{22}(r,0) = \frac{\sigma_\infty a}{\sqrt{r}\sqrt{2a}} = \frac{\sigma_\infty\sqrt{a}}{\sqrt{2r}}. \qquad (2.79)$$

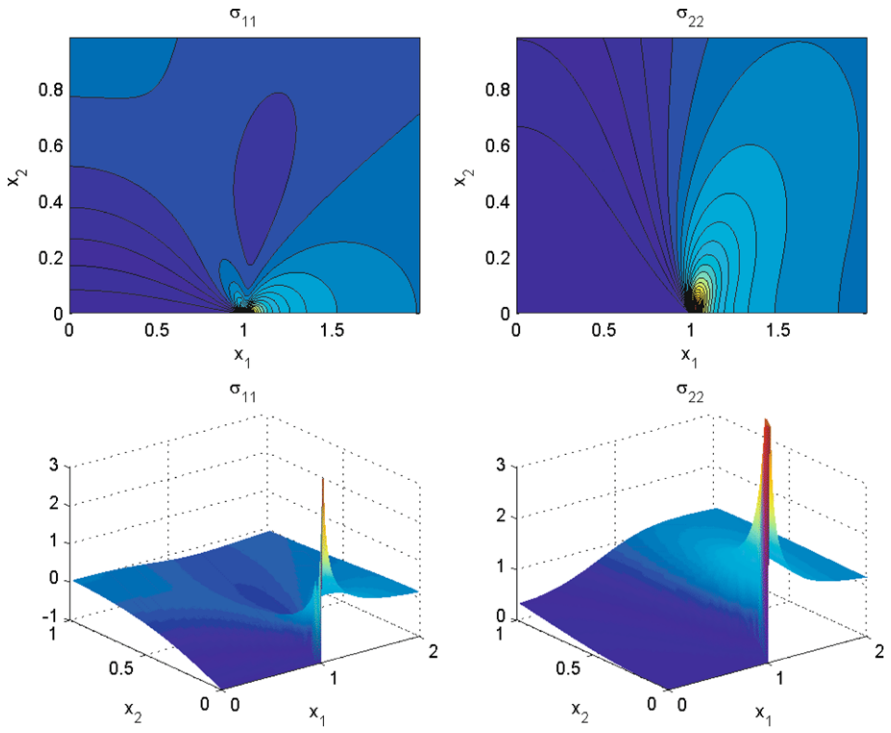

Fig. 2.8 Stress fields for finite crack in an infinite plate under tension. Stress normalized by σ_∞, coordinates normalized by a, from Eq. (2.78)

Using the definition of stress intensity factor, $K_I = \lim_{r\to 0} \sigma_{22}(r,0)\sqrt{2\pi r}$ we find

$$K_I = \sigma_\infty \sqrt{\pi a}. \tag{2.80}$$

The opening displacement along the crack line can be found using Eq. (2.70) with ϕ' and ϕ as calculated above. The result is

$$u_2^+(x_1,0) - u_2^-(x_1,0) = \sigma_\infty \frac{\kappa+1}{4\mu}\sqrt{a^2 - x_1^2}. \tag{2.81}$$

2.6.5 Stress Intensity Factor Under Remote Shear Loading

Similarly it can be shown that for a crack subject to remote stresses, $\sigma_{11} = 0$, $\sigma_{22} = 0$, $\sigma_{12} = \tau_\infty$ that the Mode-II stress intensity factor is

$$K_{II} = \tau_\infty \sqrt{\pi a}. \tag{2.82}$$

2.6.6 Stress Intensity Factors for Cracks Loaded with Tractions

We can develop equations for the stress intensity factors by focusing on the stresses near one crack tip. At the right hand crack tip, as $z \to a$, $z + a \approx 2a$, and $z - t \approx a - t$, hence from Eq. (2.73)

$$\phi' = \frac{1}{\pi} \frac{1}{\sqrt{z-a}} \frac{1}{\sqrt{2a}} \int_{-a}^{a} p_2(t) \sqrt{\frac{a+t}{a-t}}\, dt. \tag{2.83}$$

Using $\sigma_{22} = \mathrm{Re}\,\phi' + x_2 \,\mathrm{Im}\,\phi'' + \sigma_\infty$ and specializing to $z = x_1$, $x_1 \geq a$, the stress ahead of the crack is

$$\sigma_{22}(x_1, 0) = \frac{1}{\pi\sqrt{2a}} \frac{1}{\sqrt{x_1 - a}} \int_{-a}^{a} p_2(t) \sqrt{\frac{a+t}{a-t}}\, dt + \sigma_\infty. \tag{2.84}$$

Using the definition of stress intensity factor as above and making the substitution $z = x_1 - a$ we find that

$$K_I = \frac{1}{\sqrt{\pi a}} \int_{-a}^{a} p_2(t) \sqrt{\frac{a+t}{a-t}}\, dt. \tag{2.85}$$

Similarly, K_{II} is given by

$$K_{II} = \frac{1}{\sqrt{\pi a}} \int_{-a}^{a} p_1(t) \sqrt{\frac{a+t}{a-t}}\, dt. \tag{2.86}$$

2.6.7 Asymptotic Mode I Field Derived from Full Field Solution

From Eqs. (2.85) and (2.83), as $z \to a$, ϕ' and ϕ'' for Mode-I loading may be written as

$$\begin{aligned} \phi' &= \frac{K_I}{\sqrt{2\pi}} \frac{1}{\sqrt{z-a}}, \\ \phi'' &= -\frac{K_I}{\sqrt{2\pi}} \frac{1}{2(z-a)^{3/2}}. \end{aligned} \tag{2.87}$$

Making the substitution $z - a = re^{i\theta}$, we have $1/\sqrt{z-a} = (1/\sqrt{r})e^{-i\theta/2} = (1/\sqrt{r})(\cos\theta/2 - i\sin\theta/2)$, and $1/(z-a)^{3/2} = (1/r^{3/2})e^{-3i\theta/2} = (1/r^{3/2})(\cos 3\theta/2 - i\sin 3\theta/2)$. Thus Eqs. (2.87) can be written as

$$\begin{aligned} \phi' &= \frac{K_I}{\sqrt{2\pi}} \frac{1}{\sqrt{r}} e^{-i\theta/2}, \\ \phi'' &= -\frac{K_I}{2\sqrt{2\pi}} \frac{1}{r^{3/2}} e^{-3i\theta/2}. \end{aligned} \tag{2.88}$$

Substituting the above into Eq. (2.69), and using $x_2 = r\sin\theta$ we obtain (using σ_{22} as an example)

$$\sigma_{22} = \frac{K_I}{\sqrt{2\pi}}\left(\frac{1}{\sqrt{r}}\cos\frac{\theta}{2} + r\ \sin\theta\frac{1}{2}\frac{1}{r^{3/2}}\sin\frac{3\theta}{2}\right).$$

Using the identity $\sin\theta = 2\sin\frac{\theta}{2}\cos\frac{\theta}{2}$, σ_{22} can be written as

$$\sigma_{22} = \frac{K_I}{\sqrt{2\pi r}}\cos\frac{\theta}{2}\left(1 + \sin\frac{\theta}{2}\sin\frac{3\theta}{2}\right). \tag{2.89}$$

The stress σ_{11} is the same but with a change in the sign of the second term,

$$\sigma_{11} = \frac{K_I}{\sqrt{2\pi r}}\cos\frac{\theta}{2}\left(1 - \sin\frac{\theta}{2}\sin\frac{3\theta}{2}\right). \tag{2.90}$$

In the same manner the shear stress is found to be

$$\sigma_{12} = \frac{K_I}{\sqrt{2\pi r}}\cos\frac{\theta}{2}\sin\frac{\theta}{2}\cos\frac{3\theta}{2}. \tag{2.91}$$

The asymptotic stress function, Eq. (2.87) can be integrated, yielding

$$\phi = \frac{K_I}{\sqrt{2\pi}}2\sqrt{z-a} = K_I\sqrt{\frac{2}{\pi}}\sqrt{r}e^{i\theta/2}. \tag{2.92}$$

Substituting Eq. (2.92) and Eq. (2.87) into Eqs. (2.70) we find (using u_2 as an example)

$$2\mu u_2 = \frac{\kappa+1}{2}K_I\sqrt{\frac{2}{\pi}}\sqrt{r}\sin\frac{\theta}{2} - r\sin\theta\frac{K_I}{\sqrt{2\pi r}}\cos\frac{\theta}{2}.$$

Collecting terms and using the identities $\sin\theta = 2\sin\frac{\theta}{2}\cos\frac{\theta}{2}$ and $2\cos^2\frac{\theta}{2} = 1+\cos\theta$ the displacement can be written as

$$u_2 = \frac{K_I}{2\mu}\sqrt{\frac{r}{2\pi}}\sin\frac{\theta}{2}(\kappa - \cos\theta). \tag{2.93}$$

Similarly

$$u_1 = \frac{K_I}{2\mu}\sqrt{\frac{r}{2\pi}}\cos\frac{\theta}{2}(\kappa - \cos\theta). \tag{2.94}$$

2.6.8 Asymptotic Mode II Field Derived from Full Field Solution

Following similar procedures the Mode-II fields can be derived in Cartesian coordinates, resulting in the stress field,

$$\begin{pmatrix}\sigma_{11}\\ \sigma_{12}\\ \sigma_{22}\end{pmatrix} = \frac{K_{II}}{\sqrt{2\pi r}}\begin{pmatrix}-\sin\frac{\theta}{2}(2+\cos\frac{\theta}{2}\cos\frac{3\theta}{2})\\ \cos\frac{\theta}{2}(1-\sin\frac{\theta}{2}\sin\frac{3\theta}{2})\\ \sin\frac{\theta}{2}\cos\frac{\theta}{2}\cos\frac{3\theta}{2}\end{pmatrix}, \tag{2.95}$$

with displacements

$$\begin{pmatrix}u_1\\ u_2\end{pmatrix} = \frac{K_{II}}{2\mu}\sqrt{\frac{r}{2\pi}}\begin{pmatrix}\sin\frac{\theta}{2}(\kappa+2+\cos\theta)\\ -\cos\frac{\theta}{2}(\kappa-2+\cos\theta)\end{pmatrix}. \tag{2.96}$$

2.6.9 Stress Intensity Factors for Semi-infinite Crack

Consider a semi-infinite crack, Fig. 2.3, loaded with tractions over a region near the crack tip. In this case, in Eq. (2.85) let $-a \to -\infty$, $a+t \to 2a$, and transform coordinates by $a' = t - a$ so that

$$\begin{aligned} K_I &= \frac{1}{\sqrt{\pi}\sqrt{a}}\sqrt{2a}\int_{-\infty}^{0}\frac{p_2(a')}{\sqrt{-a'}}\,da',\\ K_I &= \sqrt{\frac{2}{\pi}}\int_{-\infty}^{0}\frac{p_2(a')}{\sqrt{-a'}}\,da'. \end{aligned} \tag{2.97}$$

Similarly,

$$K_{II} = \sqrt{\frac{2}{\pi}}\int_{-\infty}^{0}\frac{p_1(a')}{\sqrt{-a'}}\,da'. \tag{2.98}$$

2.7 Some Comments

How do we know that the solutions chosen above correspond to "Mode-I" and "Mode-II" as illustrated in Fig. 2.2. Perhaps the best manner to see this is to consider the displacement fields along the crack faces. Analyzing the Mode-I displacement field, Eq. (2.58), the reader can see that the relative motion of the crack faces is only in the x_2 direction, i.e. there is no relative sliding of the crack faces. Analyzing the Mode-II displacement field, Eq. (2.62) the reader will see that the crack faces do not open up, and that the top and bottom crack faces slide relative to each other. The lack of crack opening in Mode-II brings up questions regarding the effect of crack

face friction on the growth of cracks loaded in Mode-II. Note also that if $K_I < 0$, Eq. (2.61) tell us that the crack faces will interpenetrate. As this is physically impossible it tells us that in such a case the crack faces will no longer be traction free, but will push against each other and effectively it will be as if there is no crack present. This would differ however, if in the unloaded state the crack had a finite opening, arising (for example) from corrosion or other effects.

Close enough to the crack tip the stress and displacement fields are completely determined by the values of K_I, K_{II}, and K_{III}. The various methods for determining these values in laboratory and real-world applications will be discussed later in this book.

What will happen if a crack is loaded in a way that both Mode-I and Mode-II are present? What if Mode-I, Mode-II and Mode-III are all three present? The crack tip stresses will be a superposition of the solutions above. The relative values of K_I, K_{II} and K_{III} will depend on the loading and on the geometry of the crack and of the cracked body.

2.7.1 Three-Dimensional Cracks

Of course we do not live in a 2D world. So what will be different in 3D? As a start consider the simple problem of an edge crack in a plate under tension as shown in Fig. 2.9. The crack front is straight through the thickness of the plate. The stress field details for this problem were studied using a multi-grid, 3D finite element analysis [9]. This is a pure mode-I problem. The results show that the in-plane stresses, σ_{11}, σ_{22} and σ_{12} are nearly constant through the thickness with the normal stresses dropping off by approximately 25% at the free surfaces. Thus the 2D stress fields provide an accurate description of the 3D problem.

However the out-of-plane stress, σ_{33} has considerable variation through the thickness. This is to be expected. In the center of the plate, very near the crack tip, the free surfaces appear to be infinitely far away relative to the distance to the crack front and thus it is expected that the stress state will be plane-strain in which the out-of-plane normal strain and stress are $\gamma_{33} = 0$ and $\sigma_{33} = \nu(\sigma_{11} + \sigma_{22})$. At the free surfaces plane stress conditions are expected with normal stress σ_{33} and normal strain $\gamma_{33} = -\nu(\gamma_{11} + \gamma_{22})$. Note that in the plane stress solution since γ_{33} will be singular, the out-of-plane displacement, u_3 would be infinite as $r \to \infty$! Not a physically realistic result. The variation of σ_{33} through the thickness along a line perpendicular to the plate and located 45° to the x_1 axis at different distances to the crack tip is shown in Fig. 2.10. The results show that in the center of the plate, very close to the crack tip, the stress field is plane strain. Further away from the crack, $r \approx 0.33B$ the field is plane stress. Very close to the crack tip plane strain predominates except in a boundary layer near the free surfaces.

What will the stresses be at the crack line for real cracks in three dimensional objects? The stresses will be given by a superposition of the Mode-I, Mode-II and Mode-III fields with the values of K_I, K_{II} and K_{III} varying at different locations

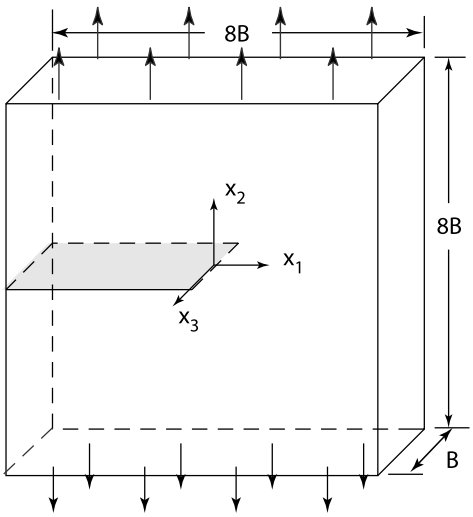

Fig. 2.9 Three-dimensional edge cracked plate loaded in tension. Adapted from [9]

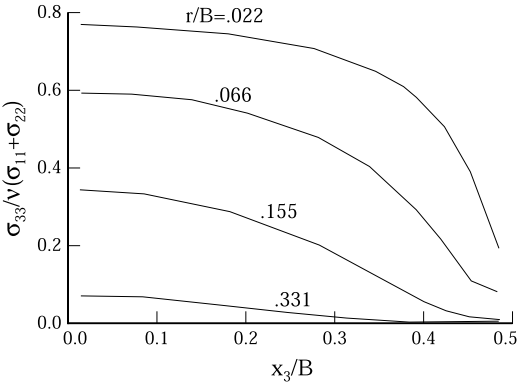

Fig. 2.10 Degree of plane strain through the plate thickness. Plots are for a line perpendicular to the plate located at $\theta = 45°$ and distances $r/B = 0.022$, 0.066, 0.155, 0.331 from the crack tip. $x_3/B = 0$ is the plate center. $x_3/B = 0.5$ is the free surface. Beyond $r \approx 0.33B$ the field is plane stress. Adapted from [9]

along the crack line. For example, consider the penny shaped crack of radius a shown in Fig. 2.11 subject to tension of σ_∞ at an angle of β to the crack surface. In this case the stress intensity factors are [10]

$$\begin{aligned} K_I &= \sigma_\infty \sqrt{\pi a} \frac{2}{\pi} \sin^2 \beta, \\ K_{II} &= \sigma_\infty \sqrt{\pi a} \frac{4}{\pi(2-\nu)} \sin\beta \cos\beta \cos\theta, \\ K_{III} &= -\sigma_\infty \sqrt{\pi a} \frac{4(1-\nu)}{\pi(2-\nu)} \sin\beta \cos\beta \sin\theta. \end{aligned} \tag{2.99}$$

At what point would the crack first begin to grow? And once growing, how would the fracture surface evolve? Such questions are still the topic of active research. To

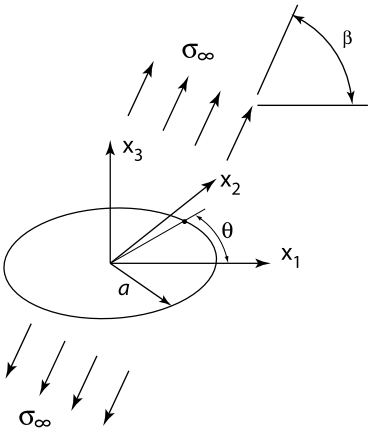

Fig. 2.11 Circular crack of radius a subject to uniform far field loading, σ_∞ at an angle of β to the crack surface. In the far-field, $\sigma_{33} = \sigma_\infty \sin^2\beta$, $\sigma_{11} = \sigma_\infty \cos^2\beta$, $\sigma_{13} = \sigma_\infty \sin\beta\cos\beta$. All other stress components are zero

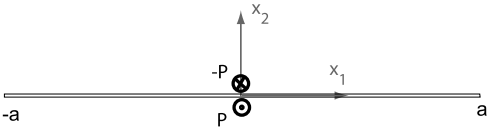

Fig. 2.12 Finite, anti-plane shear crack in an infinite body with line loads, $\pm P$ [F/L] applied

start to understand what will happen in such cases we need to study the energy flows in fracture and to address criteria for fracture. These follow in the next two chapters.

2.8 Exercises

1. Transform the Mode-III asymptotic stress field given in Eq. (2.23) into Cartesian coordinates using the appropriate coordinate transformation.
2. Using the procedure outlined in Sect. 2.4.1 determine the first term of the stress field for a crack of finite opening angle β. For what angle is the field no longer singular? Can you explain this on physical grounds?
3. Compare the asymptotic Mode-III crack tip field, Eq. (2.34) to the full-field solution Eq. (2.33) by plotting contours of the error incurred by approximating the full solution by the asymptotic solution. At approximately what distance from the crack tip does the error become greater than 10%?
4. Perform the same calculation as above for Mode-I, i.e. compare the error incurred by approximating the full-field solution for finite crack in tension with the asymptotic Mode-I field.
5. Consider a finite, anti-plane shear crack in an infinite body. Suppose that the crack is loaded by two equal and opposite line loads, P, acting on the center of the crack, as shown in Fig. 2.12. Using dimensional considerations determine how K_{III} scales with the load and crack length. Provide an intuitive explanation for this result.
6. Show that the stress function solution given in Eq. (2.43) satisfies the biharmonic equation.

7. Transform the stress field given in Eq. (2.49) into Cartesian components and verify that the Williams eigenfunction solution and the asymptotic complex variables solution, Eqs. (2.89)–(2.91) yield the same results. Show that the A_0 term corresponds to a constant stress parallel to the crack. This stress will play an important role in crack path stability and crack tip plasticity.
8. Determine the next two terms in the series solution for the Mode-I displacement field, Eq. (2.58).
9. Determine the next term in the series solution for the anti-symmetric stress field. Is there an equivalent to the constant stress term of magnitude A_0 found in the symmetric field? Why or why not?
10. Verify Eq. (2.86).
11. Using the complex variables method calculate the asymptotic Mode II stress and displacement fields.
12. Yet another way to find the asymptotic crack tip stress fields is to start with a stress function in the form of a Laurent series in z, i.e.

$$\phi = \sum A_n z^{\lambda_n}.$$

(a) Using the above as a starting point in the Westergaard approach for Mode-I, calculate the first two terms ($r^{-1/2}, r^0$) in the asymptotic stress field. (b) Do the same for the Mode-II problem.
13. Verify the integration of Eq. (2.75) leading to Eq. (2.76).
14. Verify that the stress function in Eq. (2.63) satisfies the biharmonic equation.
15. Verify Eq. (2.66) for the stress components $\sigma_{\alpha\beta}$.

References

1. C.Y. Hui, A. Ruina, Int. J. Fract. **72**, 97 (1995)
2. J.W. Brown, R.V. Churchill, *Complex Variables and Applications* (McGraw-Hill, New York, 2004)
3. M. Williams, J. Appl. Mech. **24**, 109 (1957)
4. S.P. Timoshenko, J.N. Goodier, *Theory of Elasticity* (McGraw-Hill, New York, 1969)
5. E.G. Coker, L.N.G. Filon, *A Treatise on Photoelasticity* (Cambridge University Press, Cambridge, 1931)
6. K. Hellan, *Introduction to Fracture Mechanics* (McGraw-Hill, New York, 1984)
7. H.M. Westergaard, J. Appl. Mech. **61**, A49 (1939)
8. L.I. Sedov, *A Course in Continuum Mechanics*, vol. 4 (Wolters-Noordhoff, Groningen, 1972)
9. I.D. Parsons, J.F. Hall, Eng. Fract. Mech. **33**, 45 (1989)
10. H. Tada, P.C. Paris, G.R. Irwin, *The Stress Analysis of Cracks Handbook* (ASME Press, New York, 2000)

http://www.springer.com/978-94-007-2594-2

Fracture Mechanics
Zehnder, A.T.
2012, XIV, 226 p., Hardcover
ISBN: 978-94-007-2594-2